Supporting Information

Anion induced supramolecular polymerization: a novel approach for ultrasensitive detection and separation of F^-

Qi Lin*[a], Guan-Fei Gong[a], Yan-Qing Fan[a], Yan-Yan Chen[a], Jiao Wang[a], Xiao-Wen Guan[a], Juan Liu*[b], You-Ming Zhang[a], Hong Yao[a], Tai-Bao Wei*[a]

a. Key Laboratory of Eco-Environment-Related Polymer Materials, Ministry of Education of China, Key Laboratory of Polymer Materials of Gansu Province, College of Chemistry and Chemical Engineering, Northwest Normal University, Lanzhou, Gansu, 730070, P. R. China. E-mail: linqi2004@126.com; weitaibao@126.com.

b. A College of Chemical Engineering, Northwest University for Nationalities, Lanzhou, 730070, China. E-mail: liujuan656@126.com.

Contents

Fig. S15: (a) The proposed response mechanism of **TNA** for F^- and **TNA-F** for Fe^{3+}; (b) FT-IR spectra of **TNA**, **TNA-F** and **TNA-F** + Fe^{3+} in KBr disk.

Fig. S16a: The positive ion pattern of HRMS for the **TNA-F** supramolecular polymer and simulate isotopic pattern of [**TNA**+F+K+H]$^+$.

Fig. S16b: The negative ion pattern of HRMS for the **TNA-F** supramolecular polymer and simulate isotopic pattern of [**TNA**+F+CH_3COOH]$^-$.

Fig. S17: SEM image of i): **TNA**; ii): **TNA-F**; iii): **TNA-F** + Fe^{3+}.

Fig. S18: The TEM images of the supramolecular polymer **TNA-F**.

Fig. S19: TGA curves of **TNA-F** recorded under nitrogen a heating rate of 10 °C min^{-1}.

Fig. S20: The photograph of the IC linear range.

Fig. S21: Ion chromatogram of fluoride using an eluent containing Na_2CO_3 (4.5 mM) + $NaHCO_3$ (1.4 mM), a flow rate of 1.20 mL min^{-1}, injection volume of 25 µL and suppress current of 31 mA. The peaks highlighted are due to 1-F^-. The detail data shown in **Table S2**.

Table.S2: The detailed data of **Fig. S21.**

Fig. S22: Fluorescence emission spectra for **TNA-F** (1×10^{-4} M) in DMSO/H_2O (7.4 : 2.6, v/v) solution upon the addition of 10.0 equiv. of Ca^{2+}, Mg^{2+}, Pb^{2+}, Ni^{2+}, Co^{2+}, Hg^{2+}, Zn^{2+}, Cd^{2+}, Fe^{3+}, Ag^+, Cu^{2+}, Cr^{3+}, Al^{3+}, Tb^{3+}, Ba^{2+}, La^{3+} and Eu^{3+}, respectively, (λ_{ex} = 380 nm, λ_{em} = 430 nm).

Fig. S23: Colour changes observed for **TNA-F** in DMSO/H_2O (7.4 : 2.6, v/v) solution upon the addition of 10.0 equiv. of Ca^{2+}, Mg^{2+}, Pb^{2+}, Ni^{2+}, Co^{2+}, Hg^{2+}, Zn^{2+}, Cd^{2+}, Fe^{3+}, Ag^+, Cu^{2+}, Cr^{3+}, Al^{3+}, Tb^{3+}, Ba^{2+}, La^{3+} and Eu^{3+}, respectively, under irradiation at 365 nm by a UV lamp.

Fig. S24: Fluorescence spectra of **TNA-F** (1×10^{-4} M) in the presence of different concentrations of Fe^{3+} in DMSO/H_2O (7.4 : 2.6, v/v) solution (λ_{ex} = 380 nm, λ_{em} = 430 nm).

Fig. S25: Fluorescent spectrum linear range for Fe^{3+} by addition of various concentrations of Fe^{3+} to **TNA-F** (1×10^{-4} M).

Table S3: Stability constant of iron and fluorine complexes in different proportions.

Fig. S26: Fluorescence of the sensor **TNA-F** at 380 nm with addition of 10.0 equiv. of Fe^{3+} in the presence of 10.0 equiv. of other cations in DMSO/H_2O (7.4 : 2.6, v/v) solution. (4. Ca^{2+}, 5. Mg^{2+}, 6. Pb^{2+}, 7. Ni^{2+}, 8. Co^{2+}, 9. Hg^{2+}, 10. Zn^{2+}, 11. Cd^{2+}, 12. Ag^+, 13. Cu^{2+}, 14. Cr^{3+}, 15. Al^{3+}, 16. Tb^{3+}, 17. Ba^{2+}, 18. La^{3+}, 19. Eu^{3+}).

Fig. S27: (a) A Job's plot for the **TNA** and F^-, indicating the 1 : 1 stoichiometry for **TNA-F**. (b) Fluorescent ''on-off-on'' cycles of **TNA-F**, controlled by the alternate addition of Fe^{3+} and F^-.

Fig. S28: (a) Photos of the silica gel plates loaded with **TNA** or **TNA-F** were utilized to sense F^- and Fe^{3+} in aqueous solutions under UV lamp at 365 nm; (b) Fluorescence colour changes (under the UV lamp, at λ_{ex} = 365 nm) of **TNA**-based test kit after addition of different concentration F^- aqueous solutions (from 0 M to 1×10^{-9} M).

Materials and instruments

All cations were used as the perchlorate salts, while all anions were used as the Tetrabutyl ammonium salts, which were purchased from Alfa Aesar and used as received. Fresh double distilled water was used throughout the experiment. Nuclear magnetic resonance (NMR) spectra were recorded on Varian Mercury 400 and Varian Inova 600 instruments. Mass spectra were recorded on a Bruker Esquire 6000 MS instrument. The infrared spectra were performed on a Digilab FTS-3000 Fourier transform-infrared spectrophotometer. Melting points were measured on an X-4 digital melting-point apparatus (uncorrected). The morphologies and sizes of the supramolecular polymer was characterized using field emission scanning electron microscopy (FE-SEM, UL TRA plus). The fluorescent information of the supramolecular polymer was characterized using Laser Scanning Confocal Microscope (LSCM, Olympus Fluoview FV1200). The X-ray diffraction analysis (XRD) was performed in a transmission mode with a Rigaku RINT2000 diffractometer equipped with graphite monochromated CuKa radiation (λ = 1.54073 Å). The thermal stability of the supermolecular polymer was characterized using Thermal Gravimetric Analyzer (TGA/DSC1). Fluorescence spectra were recorded on a Shimadzu RF-5301PC spectrofluorophotometer. Ion chromatography (IC) was recorded on Dionex ICS-1500.

General procedure:

1 F^- test kit preparation

The silica gel plate was been immersed in F^- solution of different concentration, then it was aired at room temperature, obtaining the **TNA** or **TNA-F** film.

2 TNA or TNA-F film preparation

The **TNA**, **TNA-F** was heated to dissolve, then, it was dumped on the silica gel plate and aired at room temperature, obtaining the **TNA** or **TNA-F** film.

3 Adsorption experiment:

Solid powder of **TNA** (10.0 mg, 1.26 x 10^{-5} mol) was suspended in a dilute aqueous solution of F^- (the concentration is about 2.61 mg/L in 10.0 mL) and stirred for 0.5 h. Then, the suspension was centrifuged at 10000 rpm for 5 min the precipitate was removed. Finally, the ingestion capacity of the **TNA** for F^- in water was assessed by ion chromatography (IC) analysis.

4 Calculate method of adsorption percentage:

Adsorption percentage (%) = $\left(1-\frac{C_1 \times V_1}{C_0 \times V_0}\right) \times 100\%$

(State: C_1 is the residual concentration of F^-, C_0 is the initial concentration of F^-, $V_1 = V_0$).

5 Calculation formula of LOD:

Linear Equation: Y = aX + b

$$\delta = \sqrt{\frac{\sum (x_i - \bar{x})^2}{n-1}}$$ (n = 20)

LOD = K × $\frac{\delta}{S}$ (K = 3, S = a × 10^6)

6 Calculation formula of association constants (K_s)

$$\ln \frac{I_x - I_{min}}{I_{max} - I_x} = \ln K_s + n\ln \left[F^-\right]$$

$$K_s = 5.46 \times 10^9$$

The stability constant (Ks) was determined by a nonlinear least squares fit of the data with the following equation as referenced elsewhere. *I* is the observed the fluorescence intensity of **TNA** at the fixed concentrations with the gradual addition of F^-. I_{max} and I_{min} are the corresponding maximum and minimum, respectively.

7 NMR experiments

(1) The host (**TNA**)-guest (F^-) ^{1}H NMR titration*:*

The **TNA** (5 mg, 1 × 10^{-2} mol) was dissolved in the DMSO-d_6 (0.5 ml), then a series of different equivalents of F^- (0.2 equiv., 0.5 equiv., 1.0 equiv.) were added into the solution of **TNA** and recorded their ^{1}H NMR respectively.

(2) The concentrations-dependent ^{1}H NMR of **TNA**:

A serious of DMSO-d_6 (0.5 ml) solutions of **TNA** with different concentrations (7.57 Mm; 12.6 mM; 17.7 mM; 27.8 mM) was prepared. Then record their ^{1}H NMR respectively.

(3) The host (**TNA**)-guest (F^-) ^{19}F NMR titration:

The tetrabutylammonium fluoride (3.8 × 10^{-5} M) was dissolved in the DMSO-d_6 (0.5 ml), then a series of different equivalents of **TNA** (0.1 equiv., 0.5 equiv., 1.0 equiv.) were added into the solution of tetrabutylammonium fluoride and recorded their ^{19}F NMR, respectively.

8 Fluorescence spectra experiments

All the fluorescence spectroscopy was carried out in DMSO/H_2O (7.4 : 2.6, v/v) solution on a Shimadzu RF–5301 spectrometer. With different equivalents tetrabutylammonium salt of anions (F^-, CN^-, I^-, Cl^-, N_3^-, ClO_4^-, $H_2PO_4^-$, AcO^-, HSO_4^-, SCN^-, Br^-) were added into **TNA** while keeping the host concentration constant (1.0 × 10^{-4} M) in all the experiments. The detection limits for guest ions were determined by fluorescent titrations and calculated on the basis of 3σ/s method.

9 Study of FT-IR spectroscopy

FT-IR spectra were recorded on a Digilab FTS-3000 Fourier transform-infrared spectrophotometer. The solid powder of **TNA**, **TNA-F** and **TNA-F** + Fe^{3+} was prepared by drying a resulting gel on a glass slice for a long time. All the samples were mixed well-distributedly with KBr to create a compact pellet for the FT-IR detection.

10 Study of scanning electron microscopy (SEM)

Determination of the SEM images was performed on a JSM-6701F FE-SEM microscope. A SEM sample was fabricated by spreading the solid powder on conductive plastic. Then gold powder was sprayed on the sample after the detection system was vacuumized. The SEM image of the solid powder was determined with an accelerating voltage of 8 kV.

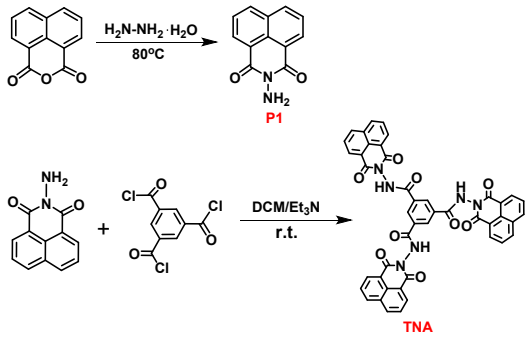

Scheme S1: Synthesis of **TNA**.

Synthesis of P1

The P1 was synthesized according to literature method[S1]. A mixture of Hydrazine hydrate (0.3182 g, 6 mmol, 80%), 1, 8-naphthalic anhydride (0.9901 g, 5 mmol) and alcohol (160.0 mL) were added to a 250 mL round-bottom flask under. The reaction mixture was stirred at 80 °C for 16 h. The solvent was removed and the residue was recrystallized in DMF and water to give the yellow needle-like solid (P1), (0.9434 g, 89%). M.P.: 265 °C. ^{1}H NMR (400 MHz, DMSO-d_6, room temperature) δ (ppm): 8.47 (m, 4H), 7.86 (t, J = 8.0 Hz, 2H), 5.78 (s, 2H). ^{13}C NMR (DMSO-d_6, 100 MHz): 160.48, 134.52, 130.80, 127.25, 126.00, 121.6. ESI-MS m/z: $[P1+H]^+$ Calcd $C_{12}H_8N_2O_2$ 213.07, found 213.00. FT-IR (anhydrous KBr, cm^{-1}) v: 3323, 3234 (NH_2), 1670 (C=O).

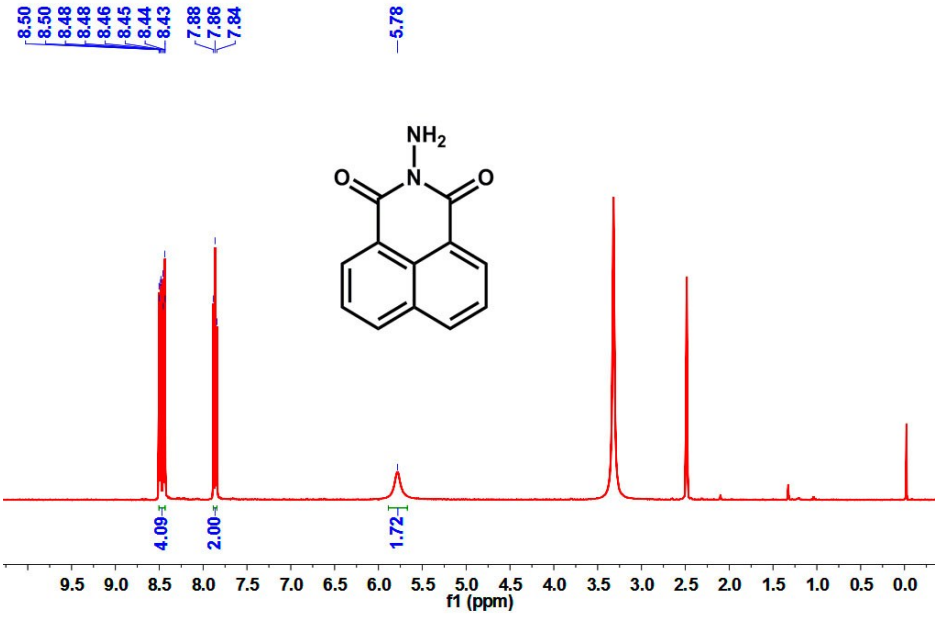

Fig.S1: ^{1}H NMR Spectrum of P1 in DMSO-d_6 (400 MHz, 298K).

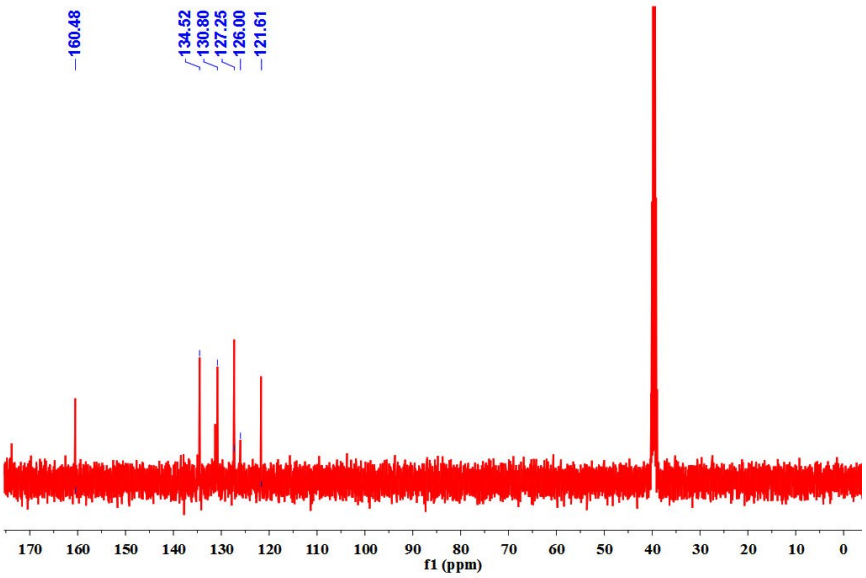

Fig.S2: ^{13}C NMR Spectrum of P1 in DMSO-d_6 (100 MHz, 298K).

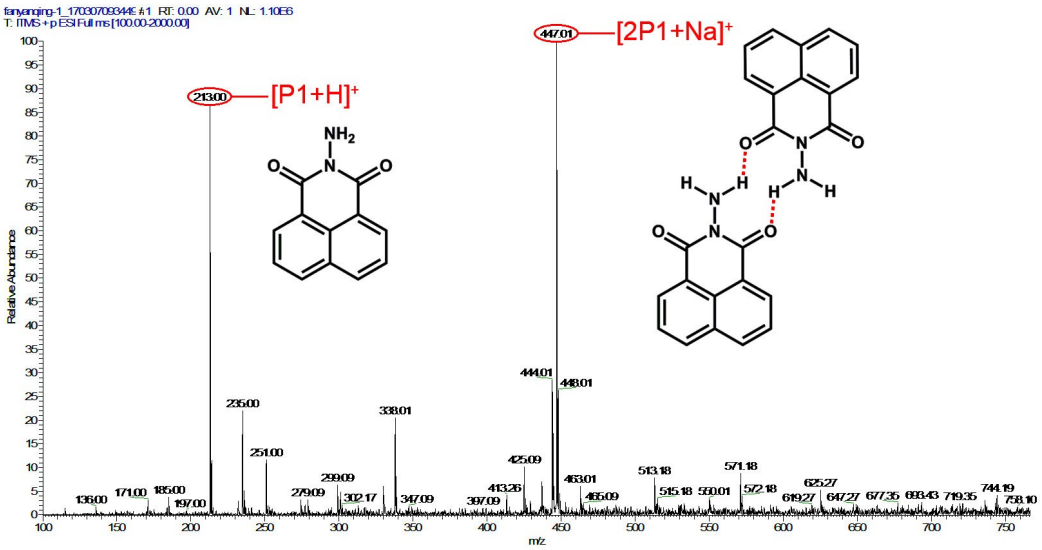

Fig.S3: ESI-MS of P1.

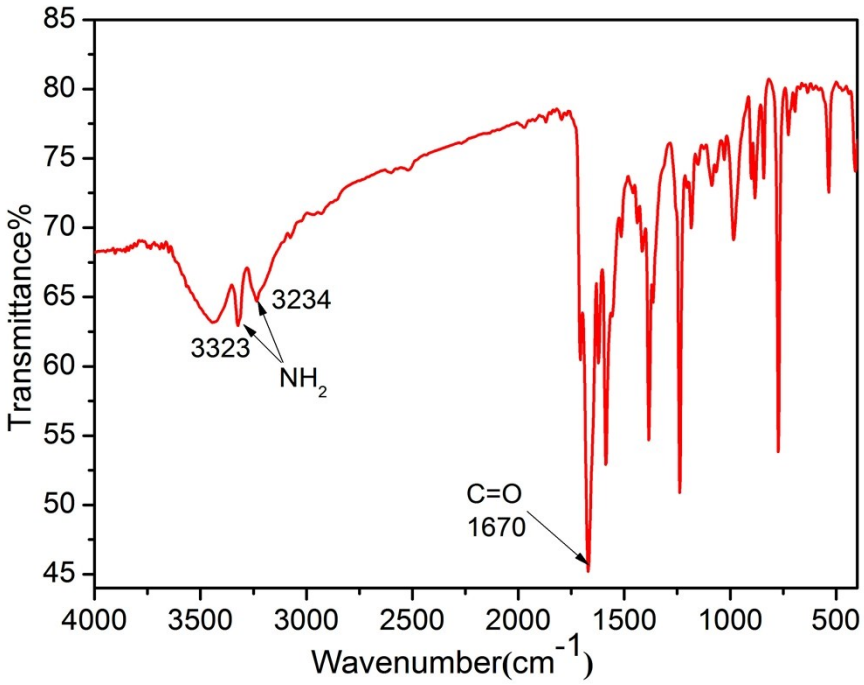

Fig.S4: FT-IR spectrum of P1 in KBr disk.

Synthesis of TNA:

A solution of 1, 3, 5-benzenetricarbonyl trichloride (1 mmol, 0.2657 g) was dropwise added into the mixture of P1 (4 mmol, 0.8482 g) and TEA (1 mL) in CH_2Cl_2. The mixture was stirred at room temperature for 15 h. The solvent was removed and the residue was recrystallized in DMF and alcohol, washed by alcohol and water. The product **TNA** was collected by filtration, and dried under vacuum (0.6256 g, 79%). M.P.: > 280 °C. ^{1}H NMR (600 MHz, DMSO-d_6, room temperature) δ (ppm): 11.81 (s, 3H), 8.84 (s, 3H), 8.58 (m, 12H), 7.94 (t, J = 6.0 Hz, 6H). ^{13}C NMR (DMSO-d_6, 150 MHz): 164.53, 162.13, 135.89, 131.95, 127.66, 121.94. HR-ESI-MS m/z: [**TNA**+Na]$^+$ Calcd $C_{45}H_{24}N_6O_9Na$ 815.1497, found 815.14972.

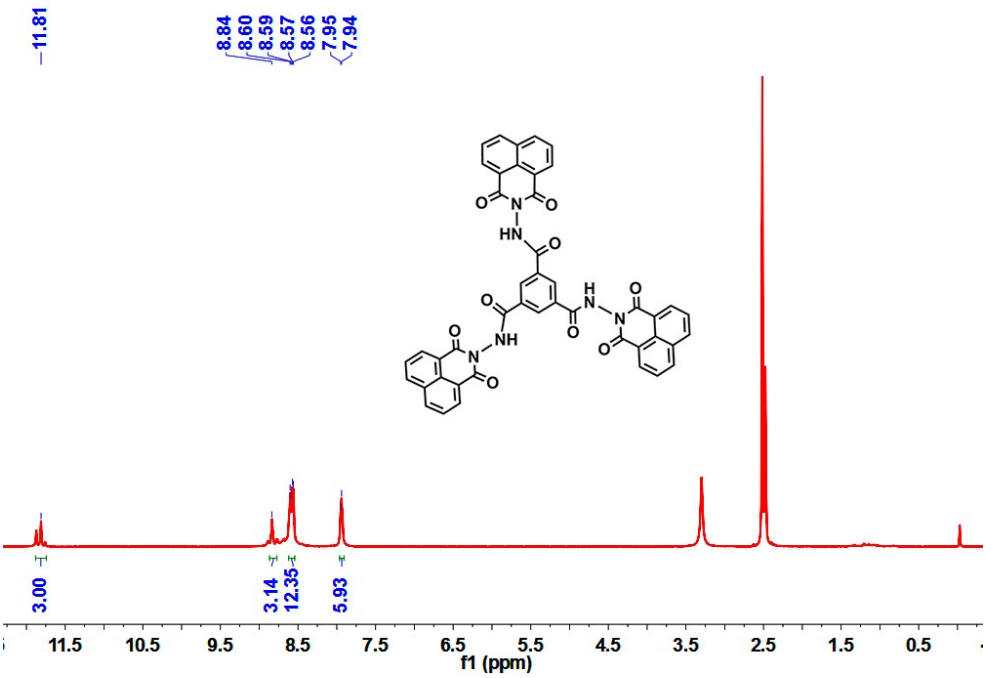

Fig. S5: ^{1}H NMR Spectrum of **TNA** in DMSO-d_6 (600 MHz, 298K).

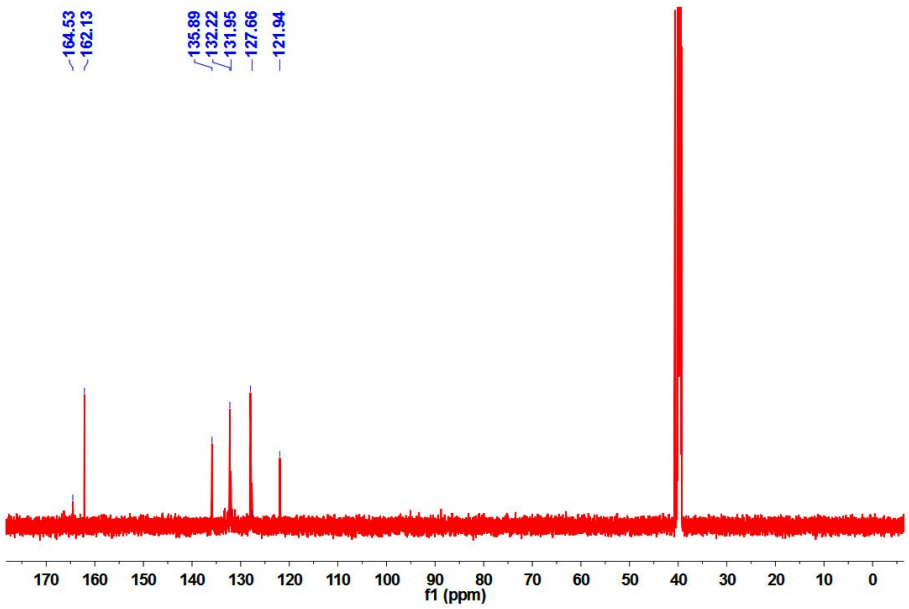

Fig. S6: ^{13}C NMR Spectrum of **TNA** in DMSO-d_6 (150 MHz, 298K).

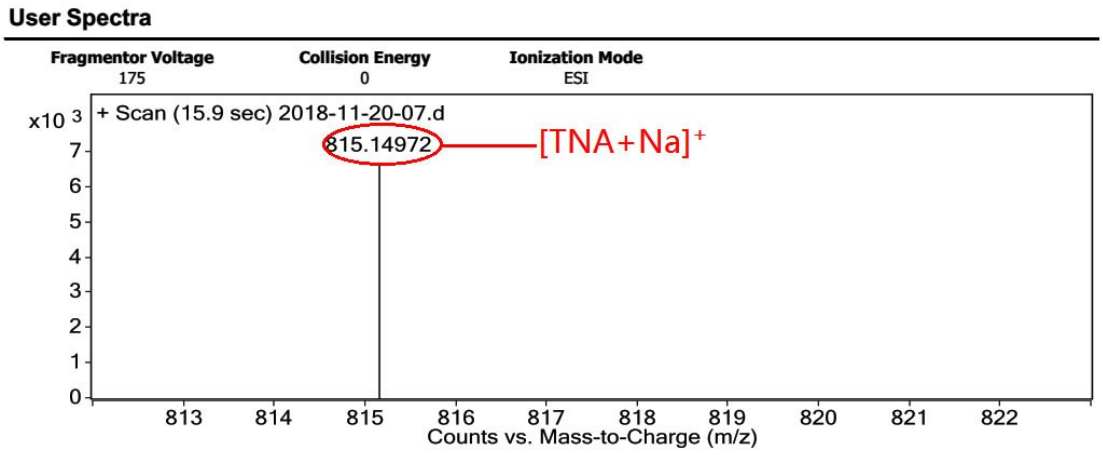

Fig. S7: HR-ESI-MS of **TNA**.

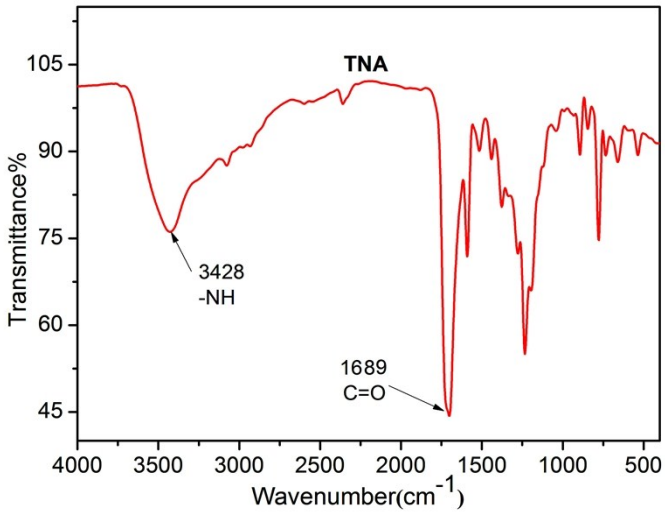

Fig.S8: FT-IR spectrum of **TNA** in KBr disk.

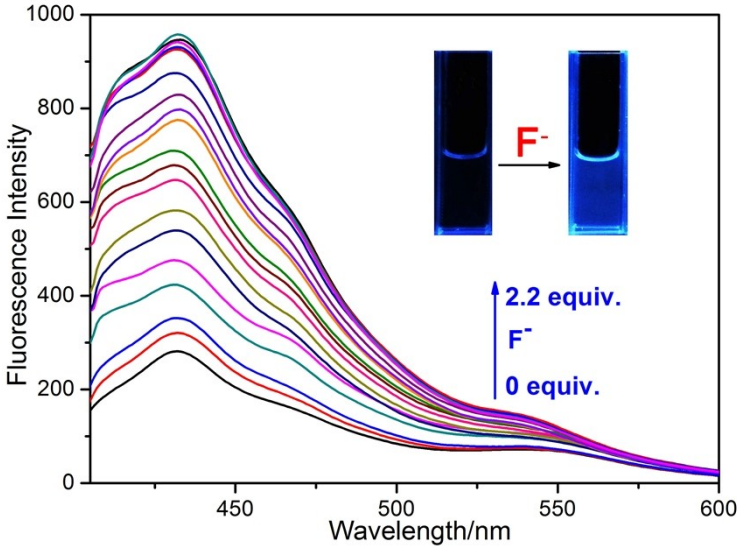

Fig. S9: Fluorescence spectra of **TNA** (1×10^{-4} M) in the presence of different concentrations of F^- in DMSO/H_2O (7.4 : 2.6, v/v) solution.

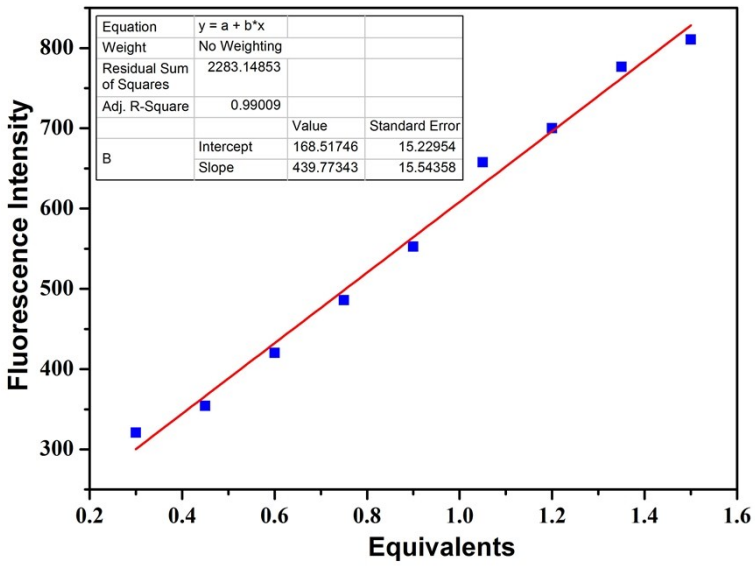

Fig. S10a: Fluorescent spectrum linear range for F^- by addition of various concentrations of F^- to **TNA** (1×10^{-4} M).

Linear Equation: Y = 439.77343X + 168.51746 R^2 = 0.99009

$S = 439.77343 \times 10^6$

$$\delta = \sqrt{\frac{\sum (x_i - \bar{x})^2}{n-1}} = 1.27 \text{ (n = 20)}$$

K = 3

$$\text{LOD} = K \times \frac{\delta}{S} = 8.67 \times 10^{-9} \text{ M}$$

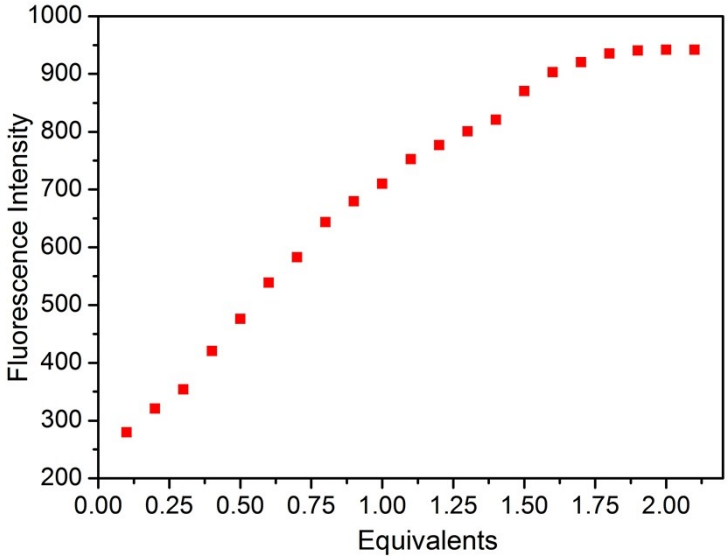

Fig. S10b: A plot of emission of **TNA** at 430 nm versus number of equivalents of F^-.

Table S1: The detection limits of reported F^- sensors based on various detection mechanism.

Ref.	Detection mechanism	Solvent	LOD(M)
[8a]	F^- induced the QD-conjugate	$CHCl_3$	7.4×10^{-7}
[8b]	F^- induced the DL-PQD aggregation	Toluene	3.2×10^{-6}
[9]	F^- induced the oxidase activity enhancement	Acetate buffer	6.4×10^{-7}
[10]	$F^-\cdots$H-N Hydrogen bond	Aqueous solution	9.7×10^{-7}
[11a]	F^- driven silyl deprotection	Acetonitrile	5.0×10^{-8}
[11b]	F^- reacted with boric acid group	DMF/H_2O (7:3)	2.0×10^{-6}
[11c]	F^- reacted with triisopropylsilyl	DMSO	1.2×10^{-7}
[12]	F^- coordination and $F^-\cdots$H-C Hydrogen bond	Aqueous solution	2.0×10^{-5}
This work	**F^- induced supramolecular polymerization**	DMSO/H_2O (7.4:2.6)	**8.7×10^{-9}**

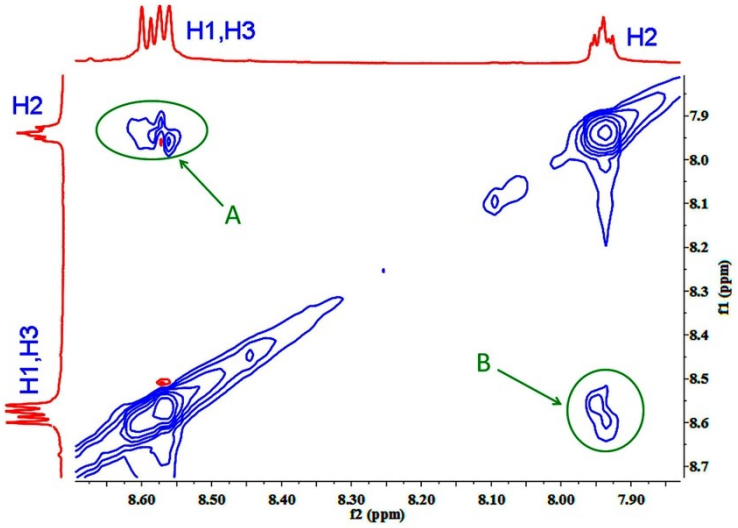

Fig. S11: 2D NOESY NMR spectrum of the supramolecular polymer fiber **TNA-F** in DMSO-d_6 solution.

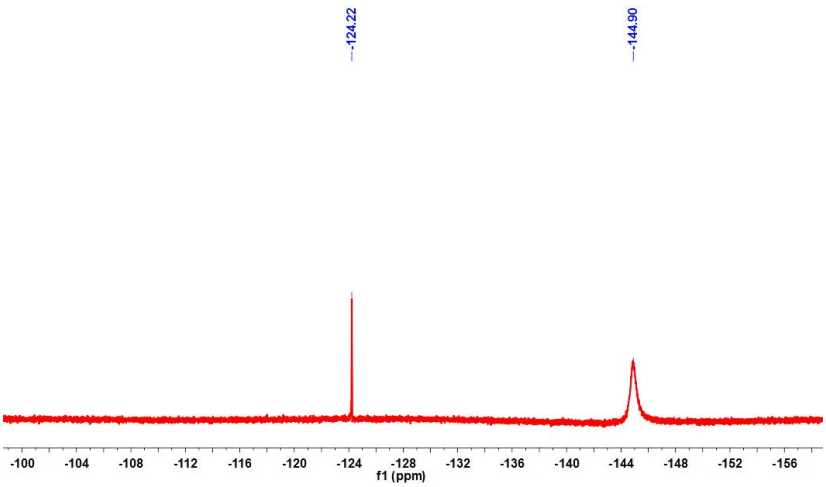

Fig. S12: The ^{19}F NMR spectrum of the supramolecular polymer fiber **TNA-F** in DMSO-d_6 (376 MHz, 298K).

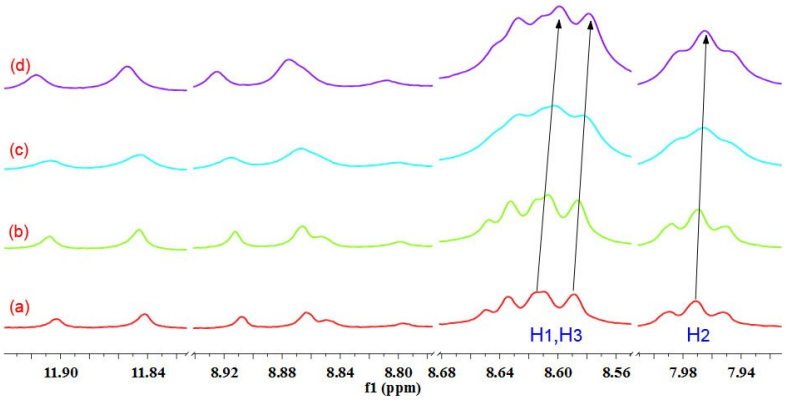

Fig. S13: Partial ^{1}H NMR spectra (400 MHz, 298 K) of **TNA** in DMSO-d_6 at various concentrations: (a) 7.57 mM, (b) 12.6 mM, (c) 17.7 mM, (d) 27.8 mM.

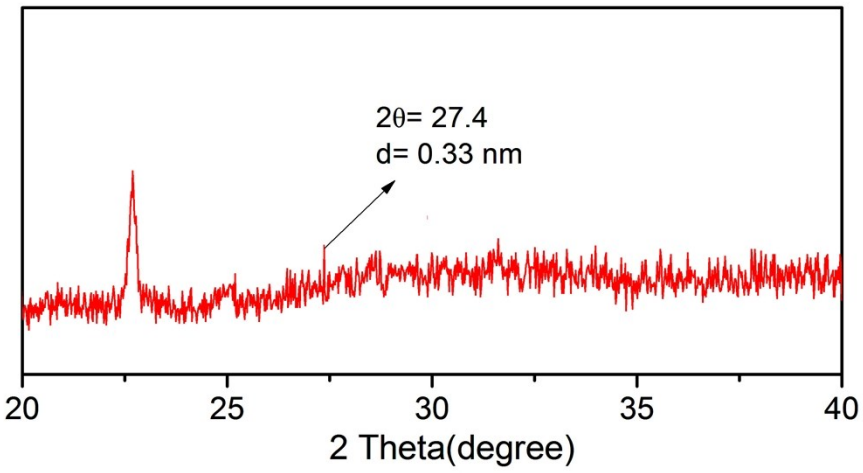

Fig. S14: XRD pattern of the **TNA-F.**

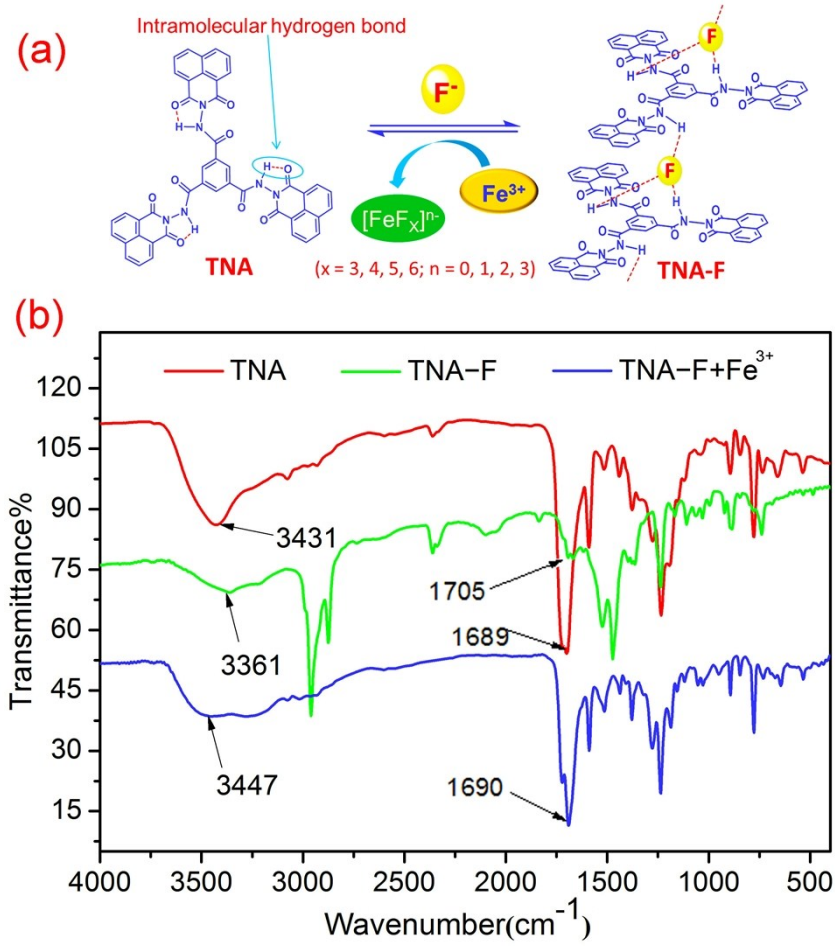

Fig. S15: (a) The proposed response mechanism of **TNA** for F^- and **TNA-F** for Fe^{3+}; (b) FT-IR spectra of **TNA**, **TNA-F** and **TNA-F** + Fe^{3+} in KBr disk.

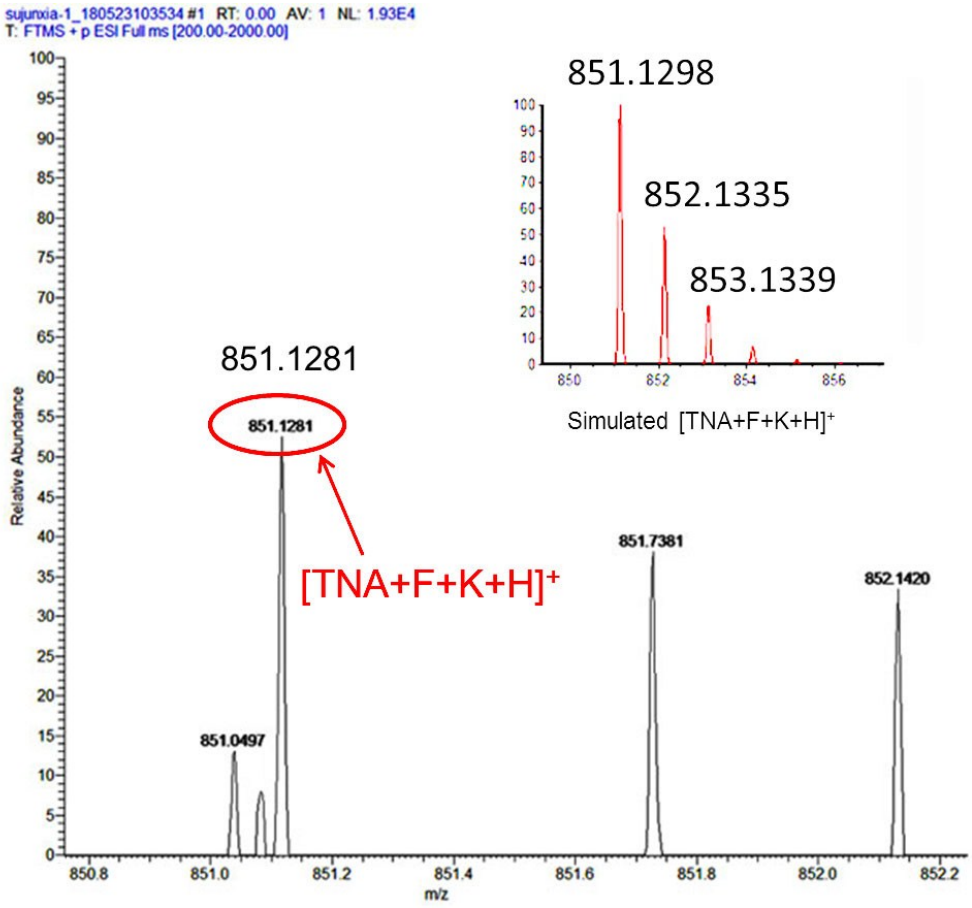

Fig. S16a: The positive ion pattern of HRMS for the **TNA-F** supramolecular polymer and simulate isotopic pattern of [**TNA**+F+K+H]$^+$.

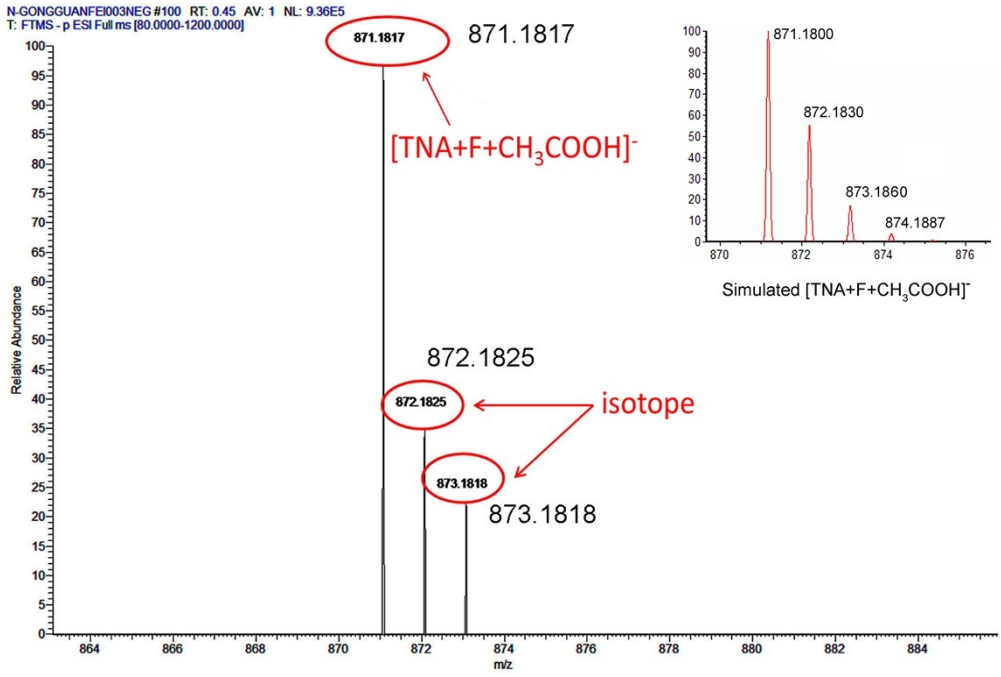

Fig. S16b: The negative ion pattern of HRMS for the **TNA-F** supramolecular polymer and simulate isotopic pattern of [**TNA**+F+CH_3COOH]$^-$.

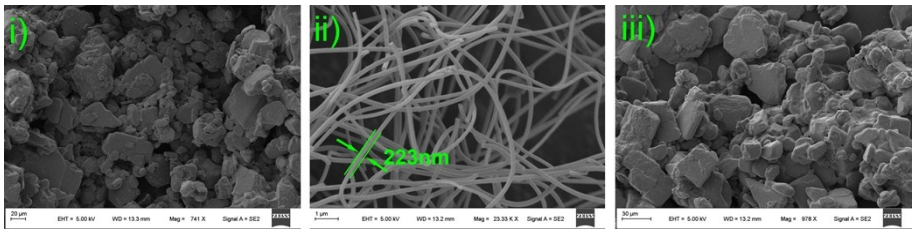

Fig. S17: SEM image of i): **TNA**; ii): **TNA-F**; iii): **TNA-F** + Fe^{3+}.

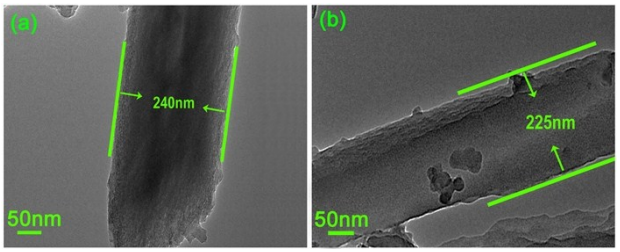

Fig. S18: The TEM images of the **TNA-F** supramolecular polymer.

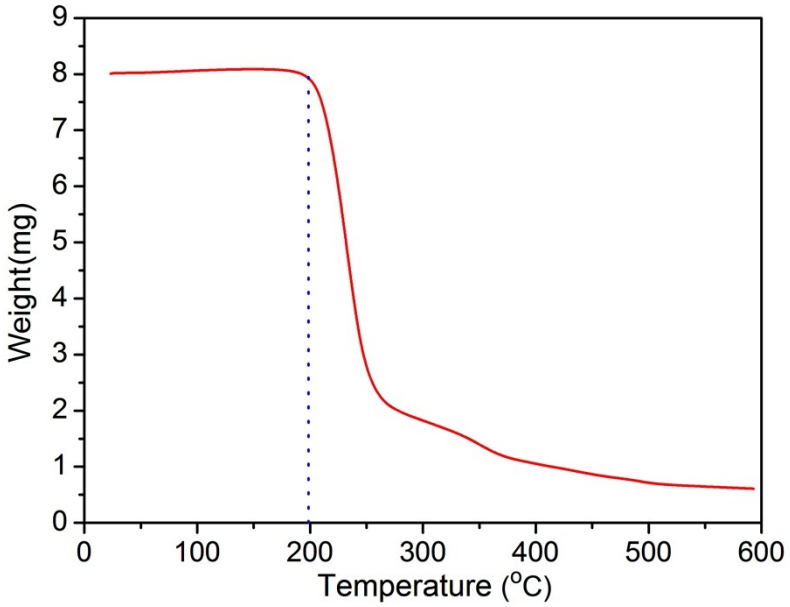

Fig. S19: TGA curves of **TNA-F** recorded under nitrogen a heating rate of 10 °C min^{-1}.

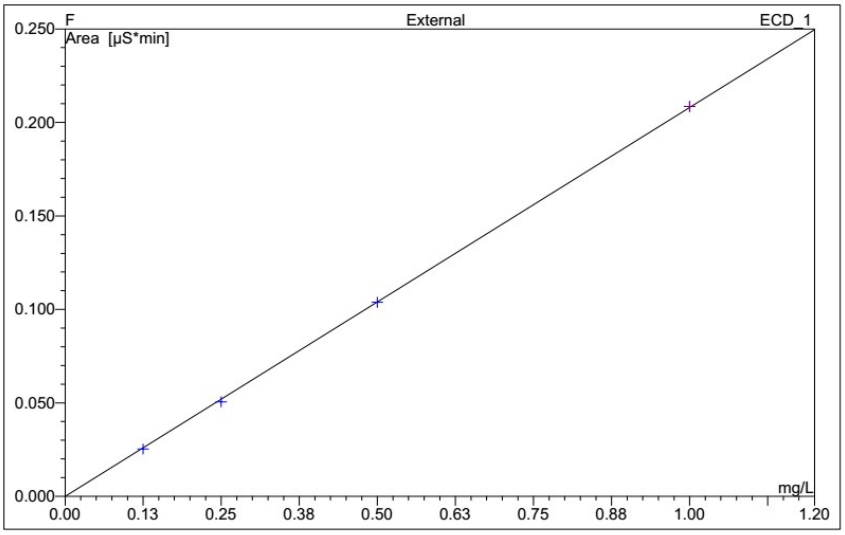

No.	Ret.Time min	Peak Name	Cal.Type	Points	Coeff.Det. %	Offset	Slope	Curve
1	3.07	F	Lin	4	99.9847	0.0000	0.2080	0.0000
Average:					99.9847	0.0000	0.2080	0.0000

Fig. S20: The photograph of the IC linear range.

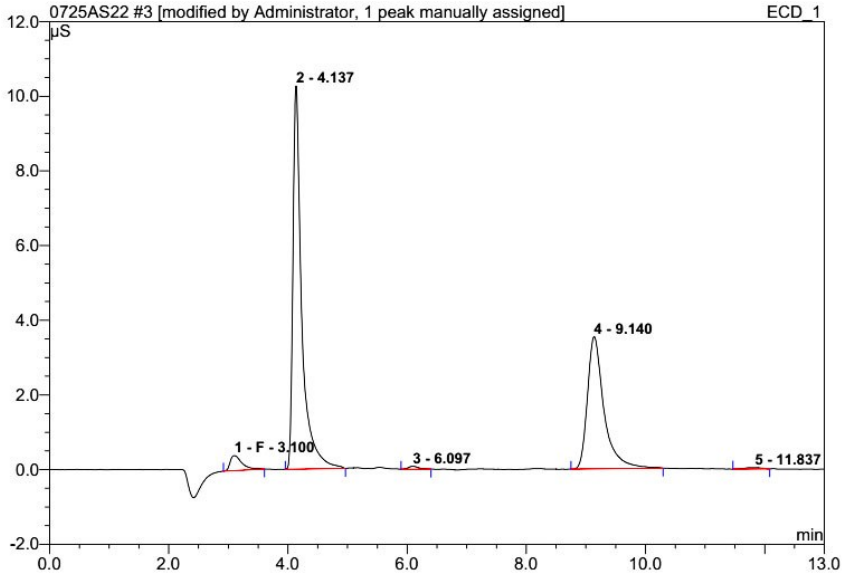

Fig. S21: Ion chromatogram of fluoride using an eluent containing Na_2CO_3 (4.5 mM) + $NaHCO_3$ (1.4 mM), a flow rate of 1.20 mL min^{-1}, injection volume of 25 µL and suppress current of 31 mA. The peaks highlighted are due to 1-F^-. Detailed Data shown in **Table S2**.

Table S2: The detailed data of **Fig. S21**.

No.	Ret.Time min	Peak Name	Height µS	Area µS*min	Rel.Area %	Amount mg/L	Type
1	3.10	F	0.399	0.092	3.07	0.400	BMB*^
2	4.14	n.a.	10.265	1.757	58.29	n.a.	BMB
3	6.10	n.a.	0.077	0.015	0.51	n.a.	BMB
4	9.14	n.a.	3.543	1.138	37.76	n.a.	BMB
5	11.84	n.a.	0.034	0.011	0.37	n.a.	BMB
Total:			14.317	3.014	100.00	0.400	

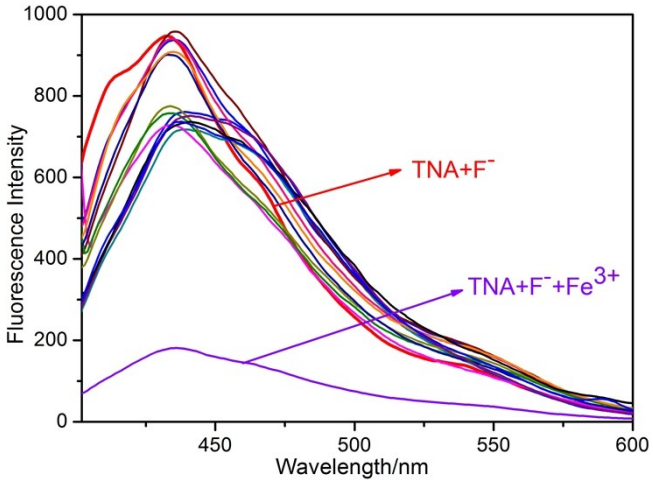

Fig. S22: Fluorescence emission spectra for **TNA-F** (1×10^{-4} M) in DMSO/H_2O (7.4 : 2.6, v/v) solution upon the addition of 10.0 equiv. of Ca^{2+}, Mg^{2+}, Pb^{2+}, Ni^{2+}, Co^{2+}, Hg^{2+}, Zn^{2+}, Cd^{2+}, Fe^{3+}, Ag^{+}, Cu^{2+}, Cr^{3+}, Al^{3+}, Tb^{3+}, Ba^{2+}, La^{3+} and Eu^{3+}, respectively, (λ_{ex} = 380 nm, λ_{em} = 430 nm).

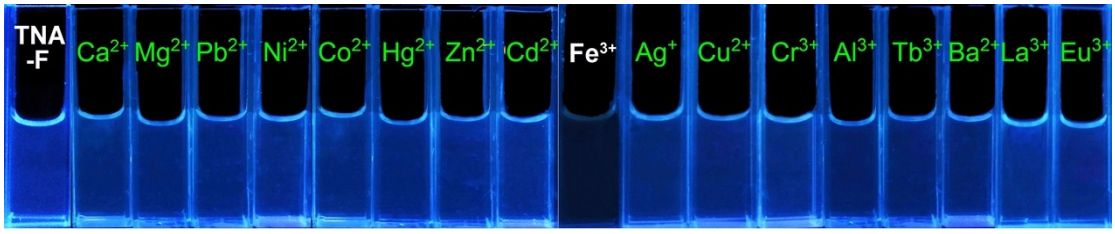

Fig. S23: Colour changes observed for **TNA-F** in DMSO/H_2O (7.4 : 2.6, v/v) solution upon the addition of 10.0 equiv. of Ca^{2+}, Mg^{2+}, Pb^{2+}, Ni^{2+}, Co^{2+}, Hg^{2+}, Zn^{2+}, Cd^{2+}, Fe^{3+}, Ag^{+}, Cu^{2+}, Cr^{3+}, Al^{3+}, Tb^{3+}, Ba^{2+}, La^{3+} and Eu^{3+}, respectively, under irradiation at 365 nm by a UV lamp.

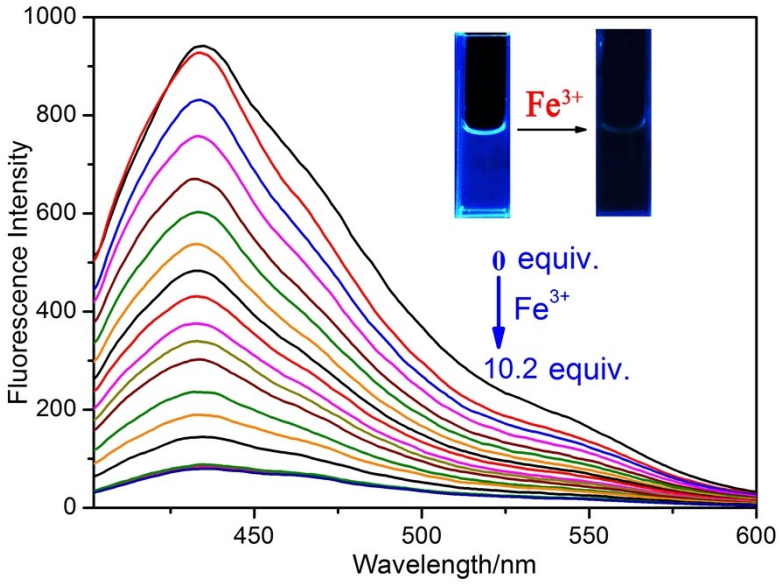

Fig. S24: Fluorescence spectra of **TNA-F** (1×10^{-4} M) in the presence of different concentrations of Fe^{3+} in DMSO/H_2O (7.4 : 2.6, v/v) solution (λ_{ex} = 380 nm, λ_{em} = 430 nm).

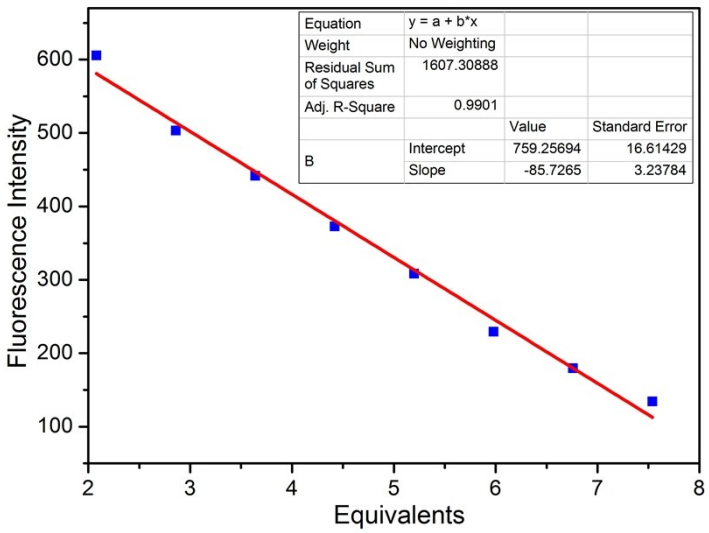

Fig. S25: Fluorescent spectrum linear range for Fe^{3+} by addition of various concentrations of Fe^{3+} to **TNA-F** (1×10^{-4} M).

Linear Equation: Y = -85.7265X + 759.25694

$R^2 = 0.9901$

$S = 85.7265 \times 10^6$

$$\delta = \sqrt{\frac{\sum (x_i - \bar{x})^2}{n-1}} = 2.73 \ (n = 20)$$

K = 3

$$LOD = K \times \frac{\delta}{S} = 9.55 \times 10^{-8} \text{ M}$$

Table S3: Stability constants of iron and fluoride complexes in different proportions.[S2 ~ S3]

Ions	Ks_1	Ks_2	Ks_3	Ks_4	Ks_5	Ks_6
Fe^{3+}	$10^{5.28}$	$10^{9.30}$	$10^{12.06}$	/	$10^{15.77}$	10^{16}

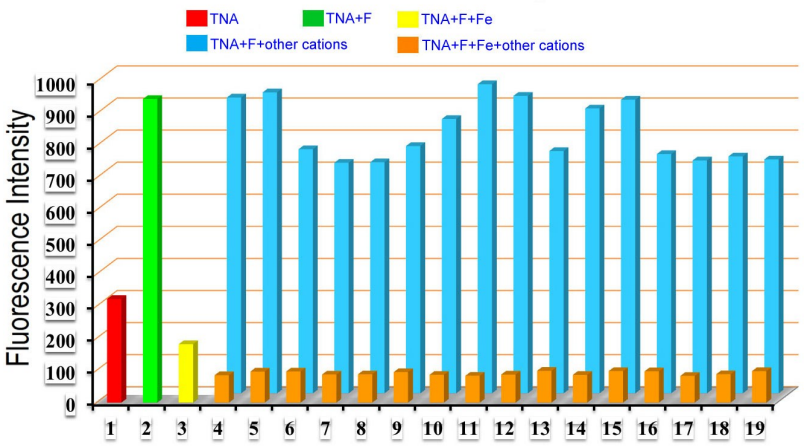

Fig. S26: Fluorescence of the sensor **TNA-F** at 380 nm with addition of 10.0 equiv. of Fe^{3+} in the presence of 10.0 equiv. of other cations in DMSO/H_2O (7.4 : 2.6, v/v) solution. (4. Ca^{2+}, 5. Mg^{2+}, 6. Pb^{2+}, 7. Ni^{2+}, 8. Co^{2+}, 9. Hg^{2+}, 10. Zn^{2+}, 11. Cd^{2+}, 12. Ag^{+}, 13. Cu^{2+}, 14. Cr^{3+}, 15. Al^{3+}, 16. Tb^{3+}, 17. Ba^{2+}, 18. La^{3+}, 19. Eu^{3+}).

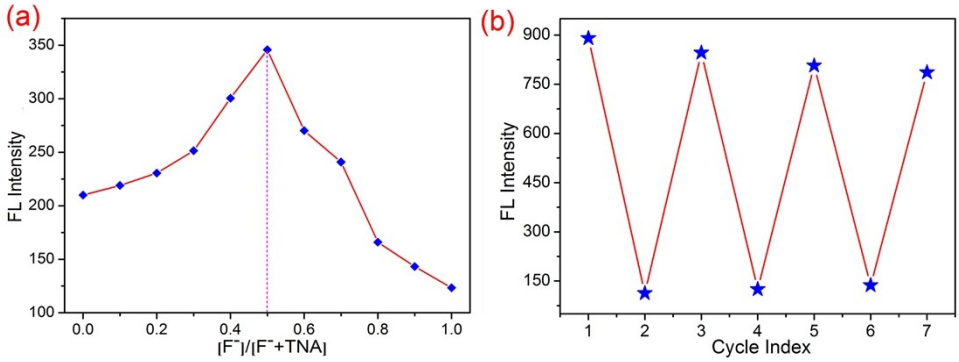

Fig. S27: (a) A Job's plot for the **TNA** and F^-, indicating the 1 : 1 stoichiometry for **TNA-F**. (b) Fluorescent ''on-off-on'' cycles of **TNA-F**, controlled by the alternate addition of Fe^{3+} and F^-.

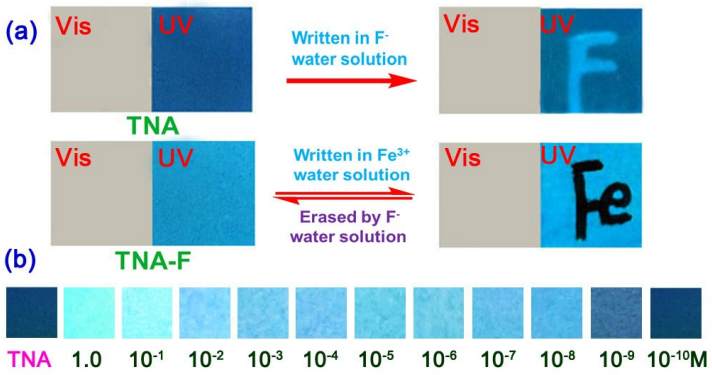

Fig. S28: (a) Photos of the silica gel plates loaded with **TNA** or **TNA-F** were utilized to sense F^- and Fe^{3+} in aqueous solutions under UV lamp at 365 nm; (b) Fluorescence colour changes (under the UV lamp, at λ_{ex} = 365 nm) of **TNA**-based test kit after addition of different concentration F^- aqueous solutions (from 0 M to 1×10^{-9} M).

Notes and references

S1: (a) C. Chen, S. Q. Shen, L. L. Dong, J. J. Zhang, Q. Yang. *Bioorganic & Medicinal Chemistry,* 2018, **26**, 394–400.

(b) P. Raj, A. Singh, A. Singh, N. Singh**.** *Dalton Trans.*, 2017, **46**, 985-994.

S2: Wuhan University Edit, *Analytical Chemistry,* Publ. 3, Higher Education Press, Beijing, 1995, pp. 526.

S3: Beijing Normal University Edit, *Inorganic Chemistry Experiment*, Publ. 2, Higher Education Press, Beijing, 1991, pp.270.